Multiple magnetic phase transitions in single-crystal $(Sr_{1-x}Ca_x)_3Ru_2O_7$ for $0 \leqslant x \leqslant 1.0$

G. Cao, S. C. McCall, and J. E. Crow

National High Magnetic Field Laboratory, Florida State University, Tallahassee, Florida 32310

R. P. Guertin*

Physics Department, Tufts University, Medford, Massachusetts 02155
(Received 12 March 1997; revised manuscript received 9 May 1997)

$Sr_3Ru_2O_7$ is a highly correlated narrow d-band metallic ferromagnet with a Curie temperature $T_C = 105$ K. $Ca_3Ru_2O_7$, which is isomorphic to $Sr_3Ru_2O_7$, becomes antiferromagnetic and remains metallic below $T_N = 56$ K and exhibits a lower-temperature transition at $T_M = 48$ K into a nonmetallic antiferromagnetic phase. Both systems have the $Sr_3Ti_2O_7$ staggered double-layered body-centered-tetragonal structure, $Ca_3Ru_2O_7$ being less ideal because of the smaller Ca ionic radius. Both systems demonstrate a very high degree of anisotropy of the magnetic and electrical properties. Magnetization and magnetic susceptibility studies for $2 < T < 400$ K and $0 < H < 7$ T, electrical resistivity for $1 < T < 300$ K, and heat capacity measurements for $1 < T < 20$ K are presented on as-grown single crystals of $(Sr_{1-x}Ca_x)_3Ru_2O_7$, spanning the full concentration range $0 \leqslant x \leqslant 1.0$. The results show multiple magnetic phases, from ferromagnetism for $x < 0.4$ to antiferromagnetism for $x > 0.4$. The transition from ferromagnetism to antiferromagnetism precedes a crossover from metallic conductivity at low temperatures to nonmetallic conductivity for $x > 0.7$ and $T \leqslant 40$ K. In all cases the resistivity at room temperature is large ($\rho \approx 0.02 - 0.04$ Ω cm), but with a metallic temperature dependence ($d\rho/dT > 0$), indicating the materials are probably ''bad'' metals. Resistivity anomalies at the transition temperatures suggest the opening of a gap at the Fermi surface for the metallic antiferromagnetic phase ($0.4 < x < 0.7$). The gap appears to evolve smoothly with increasing Ca content and may be relevant to a Mott-like metal to nonmetal transition for Ca-rich samples, $x \leqslant 1.0$. Magnetic anisotropy measurements show that the easy axis (c axis for $x = 0$) rotates into the ab plane with increasing Ca concentration and a lower-temperature canted magnetic structure is suppressed as the system becomes antiferromagnetic. The electronic component of the heat capacity, which is large for the end members of the $(Sr_{1-x}Ca_x)_3Ru_2O_7$ series, $\gamma = 77$ mJ/mole K^2 for $x = 0$ and $\gamma = 35$ mJ/mole K^2 for $x = 1.0$, is even larger for most of the mixed systems, $x \neq 0, 1.0$. The data are discussed relative to the physics of bad metals and to the highly correlated nature of the Ru-dominated narrow $4d$ bands. The results are compared with a recent analogous study of metallic ferromagnetism in single-crystal $Sr_{1-x}Ca_xRuO_3$. Included in this paper is a discussion of the strikingly strong variation between the magnetic and electrical properties of single-crystal materials compared to similar data from isostructural polycrystalline materials. [S0163-1829(97)04433-0]

I. INTRODUCTION

Electron-electron correlations often dominate band-structure effects and govern the magnetic and transport properties of metallic transition-metal oxide systems, including those of the $4d$ transition-metal ruthenium where the d bands tend to be narrow.[1] The low-temperature properties of the ruthenates span the spectrum from good metals to bad metals to magnetic insulators, where in ''bad'' metals the apparent mean free path at high temperatures for single-quasiparticle scattering is comparable to interatomic distances. Based on our own work and the work of others, very small chemical substitutions in the cation sublattices can precipitate dramatic changes in the ground states of the Ru transition-metal oxides: from paramagnetic to magnetically ordered, from metallic to nonmetallic. The boundary between bad metals and magnetic insulators is well demonstrated by the results presented in this paper.

The origin of the strong magnetism of the ruthenates lies in the localized yet strongly covalent Ru $4d$ shell. In the octahedral Ru $O6$ symmetry characteristic of many transition-metal oxides, the crystal-field interaction splits the fivefold degenerate d-shell configuration into a ground-state t_{2g} triplet, with an excited (and for Ru oxides unpopulated) doublet e_g. The t_{2g}-e_g splitting for the $4d$ systems is very large because of the large radial extent of the $4d$ shell. Consequently, the t_{2g} orbitals are filled first, which is the ''low-spin'' configuration ($S = 1$ for Ru). The exchange terms favoring parallel spin arrangements are less important. For most $3d$ oxides, where the crystal-field interaction is weaker, it is energetically favorable to fill the orbitals with parallel spins, the ''high-spin'' configuration ($S = 2$ for nd^4). The intra-atomic Coulomb interaction U in the $4d$ and $5d$ oxides is generally smaller than in the $3d$ oxides because of the larger radial extent of the d shells. From the perspective of the Mott-Hubbard model, the $4d$ and $5d$ oxides should thus be more metallic, and indeed all of the $(Sr_{1-x}Ca_x)_3Ru_2O_7$ materials are metallic, at least at room temperature.

The materials described in this paper are members of the Ruddlesden-Popper (RP) structure series for transition-metal oxides, which are characterized by the expression $A_{n+1}M_nO_{3n+1}$, $n = 1 - \infty$. Here A is an alkali- or alkaline-earth metal and M is a $3d$, $4d$, or $5d$ transition metal.[2] The index n denotes the number of coupled M-O planes in the

repeated structure and for $n=\infty$, the AMO_3 composition, the structure is perovskite based with an infinite stacking of M-O planes, the structure for colossal magnetoresistance materials, like the manganates, such as $La_{1-x}Sr_xMnO_3$. For $n=1$, the A_2MO_4 composition, the structure is that of the familiar single layered ''214'' high-T_c superconducting series, e.g., $(La_{1-x}Sr_x)_2CuO_4$.

In the work reported here, we examine the $n=2$ alkaline-earth series, namely, $(Sr_{1-x}Ca_x)_3Ru_2O_7$, and the entire concentration range $0 \leq x \leq 1.0$ is covered. Only well-characterized single-crystal samples are used in this paper, the materials being fully miscible. Previous papers[3,4] have described the rich array of magnetic, electrical, and thermodynamic properties of the end members of this series, i.e., $x=0$ and 1.0 compounds. Both end members were synthesized in single-crystal form in our laboratory. Single-crystal $Sr_3Ru_2O_7$ becomes ferromagnetic below $T_c=105$ K, with a subsequent spin reconfiguration (canting) for $T<66$ K.[3] It remains metallic ($d\rho/dT>0$, where ρ is the electrical resistivity) over the entire temperature range investigated, $1<T<400$ K. Single-crystal $Ca_3Ru_2O_7$ is also metallic at high temperatures, though with a large resistivity, and it becomes antiferromagnetic below $T_N=56$ K. A subsequent first-order metal to nonmetal ($d\rho/dT<0$), Mott-like transition occurs at $T_M=48$ K.[4] This work reviews the magnetic, transport, and thermodynamic properties of $(Sr_{1-x}Ca_x)_3Ru_2O_7$ and details the transition from ferromagnetism to antiferromagnetism as x increases from $x=0$ to 1.0 as well as the accompanying change from low-temperature metallic to nonmetallic behavior. In addition, low-temperature heat-capacity measurements ($1.5<T<20$ K) reveal large contributions from the electronic structure. In all cases, well-characterized single-crystal samples were studied and where appropriate the anisotropic properties were measured. The results are compared with a recent analogous study of the $n=\infty$ system, $Sr_{1-x}Ca_xRuO_3$. We include a discussion of the rather wide variation among the properties of the ruthenates that is found between single-crystal and polycrystalline materials.

II. SAMPLE PREPARATION AND EXPERIMENTAL TECHNIQUES

Single-crystal samples were made by a self-flux technique in Pt crucibles. The samples were heated to 1500 °C using off-stoichiometric quantities of RuO_2, $SrCO_3$ (and for mixed crystals the appropriate amount of $CaCO_3$), and the self-flux $SrCl_2$ and/or $CaCl_2$. The mixture was soaked at 1500 °C for 24 h, then cooled slowly to 1350 °C, and quenched quickly to room temperature. Examination of the surface of several samples under a differential interference contrast microscope in polarized light showed that the crystal morphology was uniform over the crystals. An analysis of sample cation composition was carried out with EDX scanning electron microscope (to an accuracy of about $x=\pm 0.005$) and all materials were examined with x-ray diffraction. All the diffraction peaks could be indexed to the body-centered-tetragonal $Ca_3Ti_2O_7$ structure. To the accuracy of these measurements, no additional phases were found with x-ray scattering, including any evidence for ferromagnetic $Sr_{1-x}Ca_xRuO_3$ (see the discussion of impurity phases in Sec. III). The oxygen

stability and content of the end members of the series were examined with thermogravimetric analysis (see Sec. III). Finally, the samples form small (1–2 mg) rectangular parallelepipeds, with the short dimension along the c axis (001). They remain stable in the atmosphere over long periods of time. All samples were measured in an as-grown state.

The magnetization of the samples ($2<T<400$ K, $0<H<7$ T) was determined with a Quantum Design MPMS superconducting quantum interference device system, the electrical resistivity with a conventional four-probe technique for $1<T<300$ K, and the heat capacity ($1.5<T<20$ K) with a low-mass thermal relaxation heat-capacity system having a sensitivity of about 1 μJ/K at 10 K.

III. PROPERTIES OF SINGLE-CRYSTAL VERSUS POLYCRYSTALLINE SAMPLES

We digress to emphasize an interesting aspect of these and related studies: the unusually large difference in physical properties found between single and polycrystals of the ruthenates. Two papers[5,6] recently have presented convincing evidence for antiferromagnetism in polycrystalline $Sr_3Ru_2O_7$ at about 15 K, in sharp contrast to the *ferromagnetism* at 105 K of single-crystal $Sr_3Ru_2O_7$.[3] The susceptibility of the polycrystalline samples from both groups shows the presence of $SrRuO_3$, which is ferromagnetic at $T_c=165$ K,[7,8] acknowledged by both groups to be present in the 2–3 % range. We have found a 2–3 at. % $SrRuO_3$ phase in all polycrystalline samples fabricated by our own group and, of course, no evidence for $SrRuO_3$ in single crystals. (Because $SrRuO_3$ is ferromagnetic, low-field magnetization can detect the presence of this phase of better than 2 at. %, which is slightly more sensitive than x-ray scattering.) Acknowledging the effect on the susceptibility of the impurity phase, it remains impossible to reconcile the drastically different results between single-crystal and polycrystalline $Sr_3Ru_2O_7$. For example, previous studies of polycrystalline $Sr_3Ru_2O_7$ suggest a magnetic anomaly in the vicinity of 15 K, but no magnetic anomaly of any kind can be found around $T=15$ K in our $Sr_3Ru_2O_7$ single crystals. In any case, such an anomaly would probably be masked by the bulk ferromagnetism, which sets in at a much higher temperature in single crystals. Finally, there is some agreement in a doped crystal: Close examination of the susceptibility of the polycrystalline $(Sr_{0.67}Ca_{0.33})_3Ru_2O_7$ data for Ref. 5 shows a weak anomaly around 80 K, consistent with the ferromagnetism for that composition in our single-crystal samples (see below).

In order to depict the difference between single-crystal and polycrystalline sample data, we show in Fig. 1(a) the isothermal magnetization at $T=5$ K for a single-crystal sample and polycrystalline $Sr_3Ru_2O_7$.[6] The single-crystal magnetization is an average along the three principal directions, i.e., $M(H)=\frac{2}{3}M_{H\perp c}+\frac{1}{3}M_{H\parallel c}$. The two steps to the magnetization result from the sharply increasing magnetization at very low fields for $H\parallel c$ (easy axis) and the sudden rise of the magnetization at about $H=3$ T for $H\perp c$ (hard axis). Regardless of averaging issues, which affect data only for $H<3$ T, the variance between single-crystal and polycrystalline data is compelling.
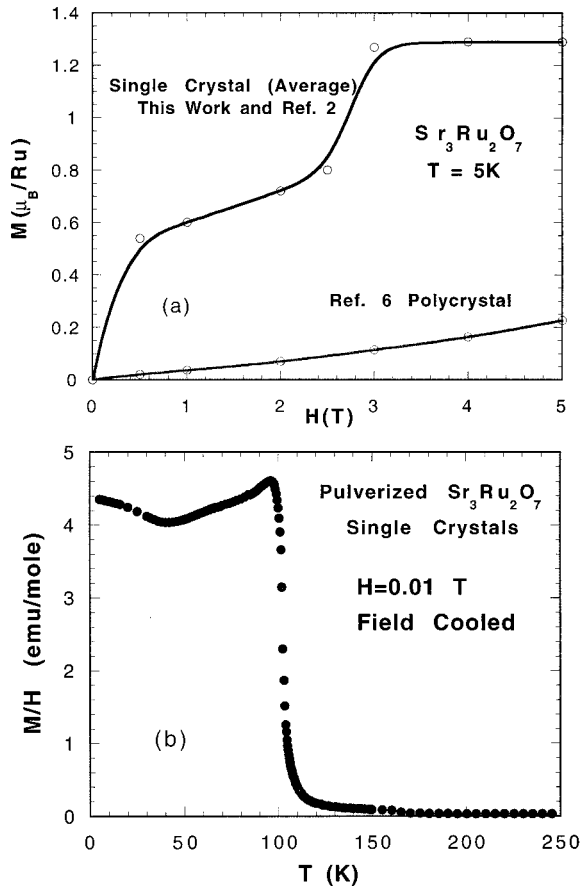
There are several additional examples of discrepancy be-

FIG. 1. (a) Comparison between the magnetization at $T = 5$ K of as-grown single-crystal ferromagnetic $Sr_3Ru_2O_7$ vs that of antiferromagnetic polycrystalline $Sr_3Ru_2O_7$ and (b) temperature dependence of the magnetic susceptibility for pulverized $Sr_3Ru_2O_7$ single crystals.

tween the properties of single-crystal and polycrystalline ruthenates: Single-crystal Sr_2RuO_4, the $n = 1$ member of the RP series, is superconducting below $T_c = 1.35$ K,[9] the first Cu-free superconductor isostructural with a high-T_c cuprate, e.g., $(La_{1-x}Sr_x)_2CuO_4$. Sr_2RuO_4 has the added feature of being superconducting in the undoped state, and there is conjecture that it may be a p-wave superconductor, analogous to liquid ^{3}He.[10] However, the authors of this discovery find that sintered samples of Sr_2RuO_4 are not superconducting.[9] Indeed, another group finds semiconducting behavior in sintered Sr_2RuO_4.[11] This behavior is unlike conventional superconductors, or high-T_c cuprate superconductors, where T_c for polycrystalline samples is generally the same as for their crystalline counterparts, if proper care is taken in preparing the samples. Another example comes from our own work with $CaRuO_3$, which shows semiconducting behavior at low temperatures as a polycrystal, but which shows metallic resistivity in single-crystal form (with a resistance ratio of near 40). Finally, the electrical resistivity of polycrystalline $Sr_3Ru_2O_7$ shows nearly-temperature-independent, slightly semiconducting behavior,[6] whereas our single crystals show clear metallic behavior, with a resistivity ratio near 10. While grain boundary effects might partially account for variations in transport, they cannot explain the drastic differences reflected in magnetic properties.

The pattern of discrepancy between single-crystal and

polycrystalline samples of the ruthenates seems too great to dismiss as simply a difference in sample quality or preparation technique. It is tempting to ascribe these differences to something more fundamental, perhaps to some very long coherence length scale in the ruthenates. One source of discrepancy could be oxygen content: Thermogravimetric analysis measurements on $Sr_3Ru_2O_7$ and $Ca_3Ru_2O_7$ showed that oxygen starts diffusing out beginning around 1100 °C and 1000 °C, respectively. Therefore, in order to test the role of oxygen content, we subjected single crystals of $Sr_3Ru_2O_7$ and $Ca_3Ru_2O_7$ to a flowing oxygen annealing at $T = 1100$ °C and 900 °C, respectively, for 1–2 days. There was no change in the Curie temperature of $Sr_3Ru_2O_7$ ($T_c = 105$ K), though the temperature of the canted phase shifted down slightly from about 66 to 53 K. However, the Mott-like transition in $Ca_3Ru_2O_7$ was fully suppressed by the oxygen annealing, meaning only the antiferromagnetic metallic state remained below $T = 56$ K in oxygenated $Ca_3Ru_2O_7$. These experiments showed that the effect of an oxygen annealing was negligible in $Sr_3Ru_2O_7$ (though not in $Ca_3Ru_2O_7$). Another source of discrepancy could be the crystallite size, but the pulverized single crystals of $Sr_3Ru_2O_7$ display a sharp ferromagnetic transition at 105 K with no trace of antiferromagnetism near 15 K [see Fig. 1(b)]. The temperature dependence of the low-field magnetization for $T \lesssim T_c = 105$ K for the pulverized single crystals is somewhat different from that measured on the single crystals.[3] This difference is expected and can be attributed to anisotropy effects that are significant for $Sr_3Ru_2O_7$ for $T > T_c$. Nevertheless, these results deepen the mystery of the huge discrepancy between single-crystal and polycrystalline $Sr_3Ru_2O_7$ by essentially eliminating both oxygen concentration and the crystallite size as contributing factors. This issue is puzzling and will be addressed further in our future work.

IV. EXPERIMENTAL RESULTS

Figure 2 shows the Ca concentration dependence of the room-temperature lattice parameters for five representative powdered $(Sr_{1-x}Ca_x)_3Ru_2O_7$ single crystals. The overall decrease in lattice parameters reflects the smaller ionic radius of Ca and more distorted structure of the Ca compound compared to the Sr compound, which is a common occurrence in other members of the RP series. At $0.33 \leq x \leq 0.69$, a plateau in the a axis is seen and may be associated with the drastic change in electronic orbitals evident in the transport properties shown below. In the similar doping regime, an anomalous Ca dependence of the a axis is also observed in polycrystalline samples.[5]

In Fig. 3 we show the electrical resistivity ρ_{ab} as a function of temperature for several $(Sr_{1-x}Ca_x)_3Ru_2O_7$ samples. In all cases the current was applied along the Ru-O planes, in the [100] or [010] direction there being no discernible difference in the resistivity between these two axes for any samples, as expected for tetragonal structures. For $Sr_3Ru_2O_7$ ($x = 0$) the sample is ferromagnetic at $T_c = 105$ K. There is no anomaly at T_c for ρ_{ab}, but a sharp decrease in the slope of ρ vs T appears at T_c for ρ_c, i.e., current measured along the c axis, which is the easy axis for magnetization in $Sr_3Ru_2O_7$ (see Ref. 3). The c axis anomaly[3] shows characteristic Fisher-Langer behavior,[12] where short-
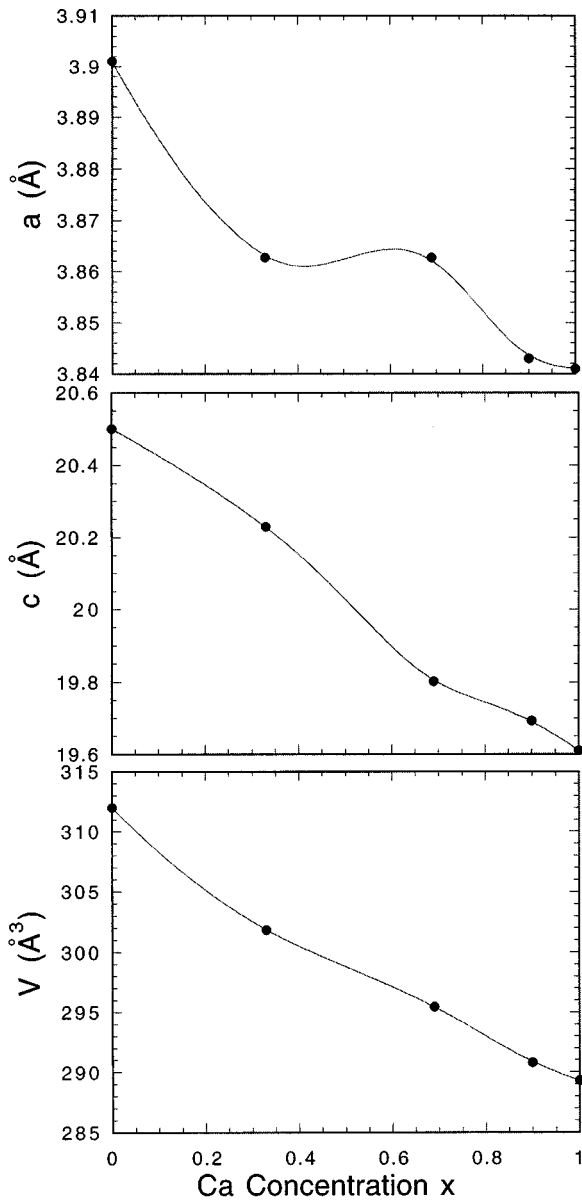
FIG. 2. Ca concentration dependence of the lattice parameters for five representative powdered single crystals.

FIG. 3. Temperature dependence of the electrical resistivity $\rho(T)$ of $(Sr_{1-x}Ca_x)_3Ru_2O_7$ showing a transition at approximately $x = 0.6$ from metallic to nonmetallic behavior. All magnetic transitions may be seen in anomalies in $\rho(T)$.

wavelength spin fluctuations dominate conduction electron scattering. The application of the Fisher-Langer model to these materials may be suspect, however, in that the model treats magnetic scattering of a single band of s-like conduction electrons from localized moments and the Ru d shell is not well localized. In addition, the carriers in the $(Sr_{1-x}Ca_x)_3Ru_2O_7$ system probably do not have s-like character.[13] Finally, the model does not treat the magnetocrystalline anisotropy associated with this system. Perhaps adjusting for the latter could explain the lack of such an anomaly for current applied perpendicular to the easy axis.

For Ca-doped materials, anomalies in ρ_{ab} resistivity begin to appear: For $x = 0.33$, there is a weak resistivity anomaly characteristic of a ferromagnetic transition for ρ_{ab} at $T_c = 80$ K, more evident in a plot of $d\rho/dT$ vs T (not shown). This suggests that as x is increased the easy axis for the magnetization rotates into the ab plane, away from the c
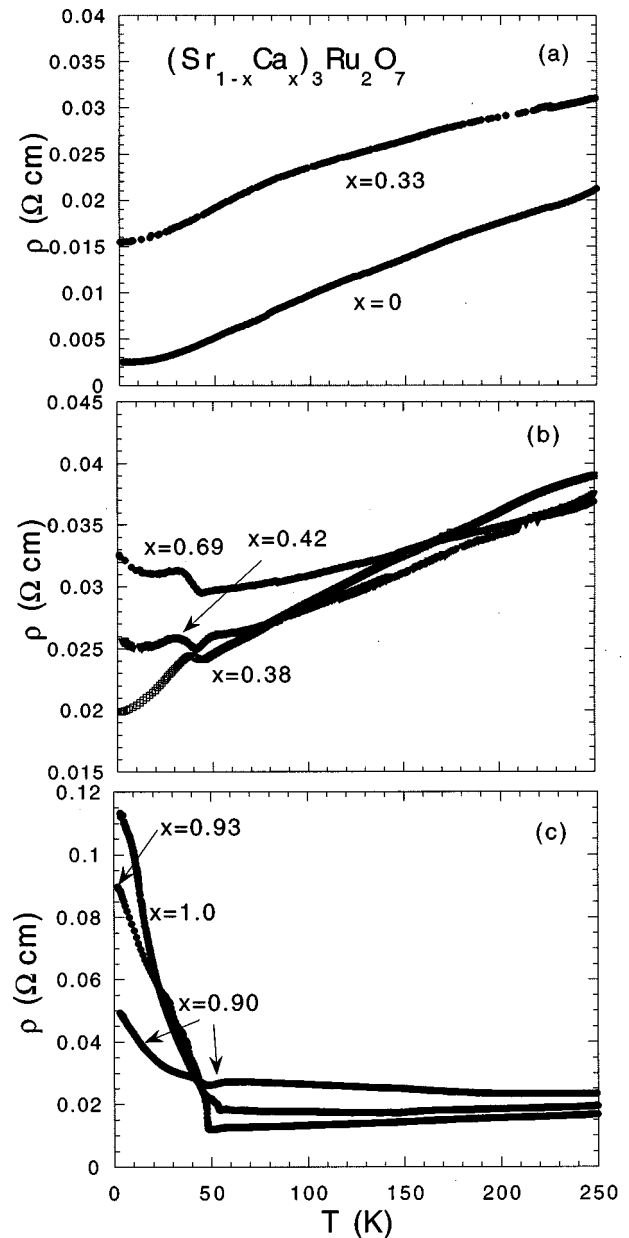
axis. (The easy axis for antiferromagnetism lies *in* the ab plane, in the [110] direction for antiferromagnetic $Ca_3Ru_2O_7$, i.e., $x = 1.0$.) We have noted previously in a related system $Sr_{1-x}Ca_xRuO_3$ (the $n = \infty$ members of the RP series) that the easy axis turns *out* of the plane with increasing x, the easy axis for ferromagnetic $SrRuO_3$ being *in* the ab plane.[8]

While the samples in Fig. 3(a) appear metallic, the resistivity for the midrange of composition $0.4 \leqslant x \leqslant 0.7$ is more complex. The temperature dependence of the resistivity $\rho(T)$ for $T > 50$ K is metallic and weakly temperature dependent [Fig. 3(b)]. For this composition range, $\rho(T)$ for $T < 50$ K becomes less metallic and an anomaly develops, which we will associate with an antiferromagnetic transition. Note that the room-temperature resistivity lies between 0.02 and 0.04 Ω cm for all the mixed samples, $x \neq 0$ or 1.0. This

is well above the resistivity ($\rho \cong 500 \, \mu\Omega$ cm) one might calculate within the Ioffe-Regel limit $k_F l \cong a$, where l is the mean free path.[14] However, this seems to be a limiting value of resistivity for the metallic phase of the $(Sr_{1-x}Ca_x)_3Ru_2O_7$ system. As x approaches 1.0 [Fig. 3(c)], the samples show nonmetallic behavior below about 40 K with increasingly sharper transitions, finally developing into a first-order metal to nonmetal, Mott-like transition in $Ca_3Ru_2O_7$ at $T_M = 48$ K. The small decrease in the resistivity at $T = 56$ K for $Ca_3Ru_2O_7$ is associated with a transition into a metallic antiferromagnetic state, as discussed in Ref. 4.

The resistive anomalies accompanying what appear to be antiferromagnetic transition temperatures for $0.38 < x < 0.69$ [Fig. 3(b)] resemble those described by the theory of Suezaki and Mori.[15] In that case a gap opens at the Fermi surface as the periodicity of the magnetic sublattice doubles in the presence of antiferromagnetic order. The appearance of some kind of gap would be consistent with the Mott-like transitions seen for more heavily doped Ca samples [Fig. 3(c)].

The behavior of the resistivity as a function of applied magnetic field for the end members of the $(Sr_{1-x}Ca_x)_3Ru_2O_7$ system, $x = 0$ and 1.0, is described in some detail in Refs. 3 and 4, respectively. We have performed a limited number of measurements of the longitudinal magnetoresistivity of some of the mixed samples. In most cases the effect of field is rather small. It is generally less than 10% at the lowest temperatures for fields to 12 T, though it reaches 18% for $Sr_3Ru_2O_7$ at $T \cong 30$ K. For the $x = 0.69$ sample, which shows an antiferromagneticlike, weakly metamagnetic transition for $T \ll T_c$ at $H = 4.5$ T along the easy axis (see below), the resistance is unchanged upon increasing H to 4 T, whereupon it drops uniformly by about 20% to $H = 12$ T, the highest field applied. This slow decrease mirrors the slow increase in magnetization at $H = 4.5$ T. Both results may be compared with $x = 1.0$, $Ca_3Ru_2O_7$, where a first-order metamagnetic increase in magnetization at $H = 6$ T from the nonmetallic to metallic phase is matched by a first-order decrease in electrical resistivity at the same field.

The temperature dependence of the low-field magnetic properties of the $(Sr_{1-x}Ca_x)_3Ru_2O_7$ system are summarized in Fig. 4. In all cases the applied magnetic field was small enough that the ''zero''-field limit in M vs H was reached, i.e., $(dM/dH)_{H \to 0}$ is linear. The multitude of magnetic transitions bears close scrutiny. The top panel Fig. 4(a) shows the distinctive step signature of ferromagnetism at $T_c = 105$ K (''kink point method'' for determining T_c). This shows clear evidence that the c axis is the easy axis because only a very small anomaly appears at T_c for $H \perp c$, i.e., $H \parallel [110]$ in Fig. 4(a).

For $(Sr_{1-x}Ca_x)_3Ru_2O_7$, $x = 0.33$ [Fig. 4(b)], T_c decreases to about 80 K, but the anomaly for in-plane magnetization grows compared to $x = 0$, indicating the easy axis rotates away from the c axis for $x > 0$. The inset of Fig. 4(b) shows a still prominent magnetization vs temperature for $H \parallel c$. As stated above, in a related system $Sr_{1-x}Ca_xRuO_3$, we found the opposite situation:[8] The easy axis (ab plane for $x = 0$) tipped *out* of the plane as Ca was substituted for Sr in ferromagnetic $SrRuO_3$ ($T_c = 165$ K). In $Sr_{1-x}Ca_xRuO_3$ ferromagnetism is also suppressed with Ca substitution. However, in the $x = 1.0$ limit, $CaRuO_3$ is an enhanced paramagnetic metal
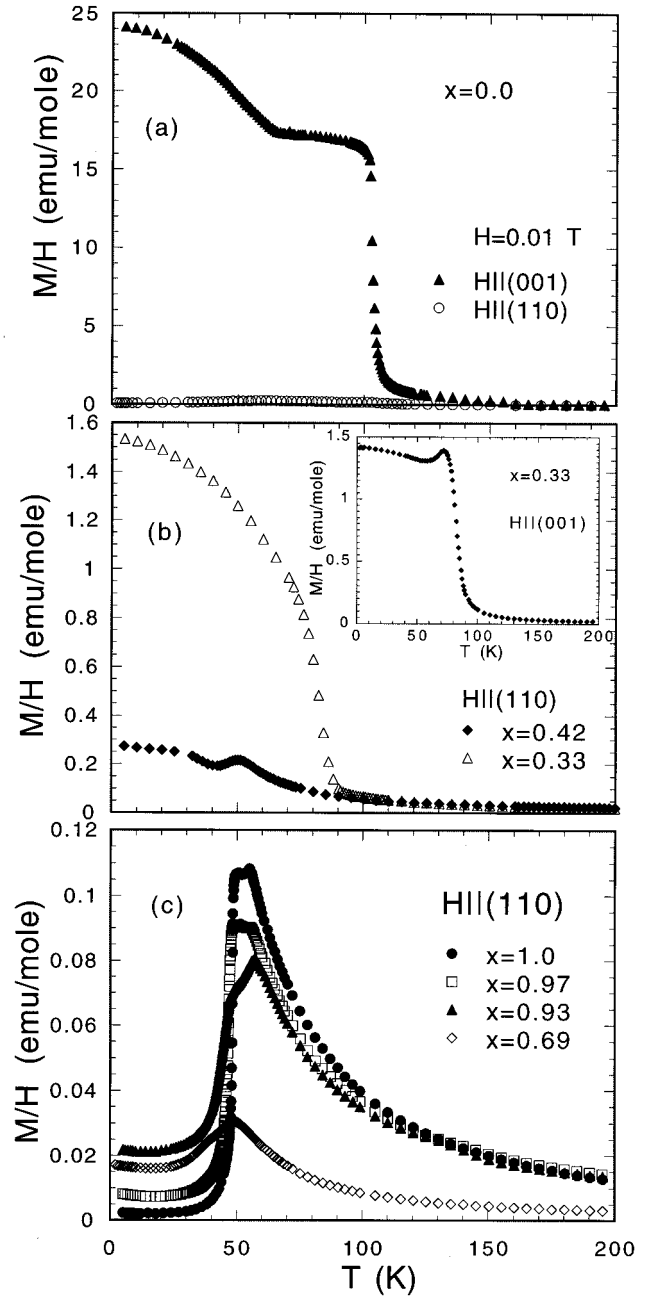

FIG. 4. Magnetic susceptibility vs temperature $M/H(T)$, for several $(Sr_{1-x}Ca_x)_3Ru_2O_7$ samples. The multiple magnetic transitions may be seen in these data and compared with the data of Fig. 2.

and does not exhibit multitransitional behavior as is seen for $Ca_3Ru_2O_7$. In $Sr_{1-x}Ca_xRuO_3$ the out-of-plane rotation was accompanied by a large increase in the magnetic hysteresis for $x > 0$.

For $x > 0.4$ [Fig. 4(c)] the transition temperature continues to decrease and becomes locked in at around 50 K. However, the shape of χ vs T develops a sharply defined peak, indicating antiferromagnetism rather than ferromagnetism. Finally, for $x = 1.0$, we see the two antiferromagnetic transitions, discussed in Ref. 3. The extremely sharp loss of moment at $T_M = 48$ K for $x = 1.0$ remains difficult to understand.

TABLE I. Parameters of fits to low-temperature heat-capacity measurements.

x	γ (mJ/mole K^2)	Θ_D (K)
0.0	77	318
0.14	192	332
0.33	170 ± 10	275
0.58	99	307
0.90	96	330
0.93	60	357
1.00	35	369

We measured the low-temperature $(1.5 < T < 20$ K$)$ heat capacity $C(T)$ of several of the $(Sr_{1-x}Ca_x)_3Ru_2O_7$ samples in an attempt to quantify the degree of d-band correlation as a function of x. This determination is complicated by the transition from metallic to nonmetallic behavior for large x: The temperature range over which the low-temperature electronic heat-capacity parameter γ was measured was in essentially the nonmetallic region for $x > 0.7$. In that case, the electronic heat capacity may measure the density of states at the Fermi surface for those regions that are not gapped as well as states within the gap. The $C(T)$ data were fit to a C/T vs T^2 dependence, where the intercept with $T = 0$ reveals γ and the coefficient of the T^2 term is a measure of the Debye temperature Θ_D. These results are tabulated in Table I.

The data from Table I and a representative fit to the C/T vs T^2 fit are shown in Fig. 5. A representative fit to the data is shown in the inset of Fig. 5(a). The general trend of γ
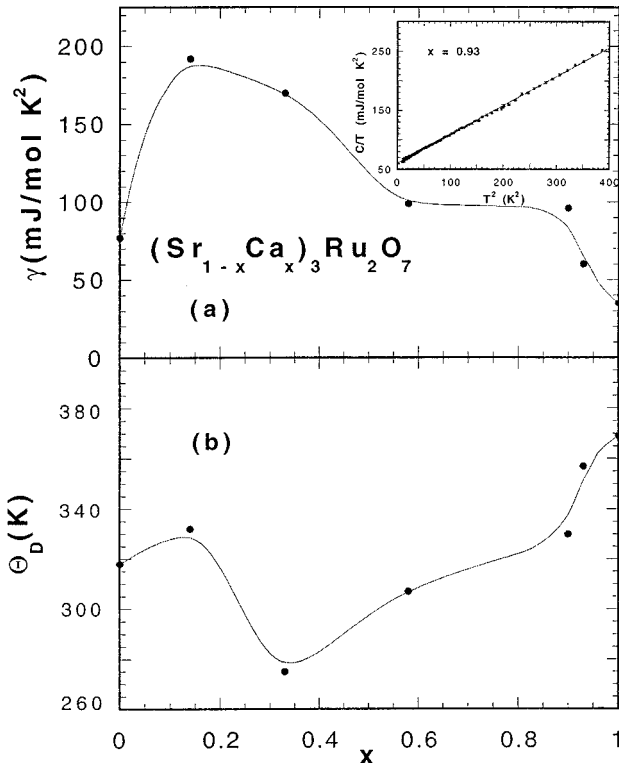

FIG. 5. Summary of fits to the heat capacity $C(T)$ vs T^2. Inset: data for a representative $(x = 0.93)$ sample.

mirrors the results obtained for the $Sr_{1-x}Ca_xRuO_3$ $(n = \infty)$ system, for $0 \leq x \leq 1.0$:[8] In $Sr_{1-x}Ca_xRuO_3$ the mixed crystals, $x \neq 0$ or 1.0, showed higher values of γ as well. The rather large rise in γ as x is decreased from 1.0 (Sr addition) may be correlated over the low-temperature range of measurement with the conductivity, which increases marginally on the approach to the metallic phase [see Fig. 3(c)]. Whether this reflects a narrowing of the d band, increased disorder, both, or some other mass enhancing mechanism is open to speculation. It is probably not a result of increased carrier concentration, as the samples tend to be more resistive in the high-temperature metallic phase, thus loosely obeying Nordheim's rule. As x is decreased from 1.0, there is also a concomitant decrease of the Mott-like transition, which disappears entirely for $x < 0.7$ as the system becomes more metallic. Attempts to include a $T^{3/2}$ term in the heat capacity resulted in improvement in some of the fits, where this term might be expected from magnon excitations, but one would expect stronger magnon contributions for lower-x samples, which was not found from fits to the data. Further analysis of the heat capacity will be pursued as these results are extended to lower temperatures, including magnetocaloric effects. This will be done to better understand the interplay between electronic and magnetic excitations.

In order to illustrate the high-magnetic-field properties, which are also useful in describing the magnetic ordering of the materials, we show in Fig. 6 the isothermal M vs $H\|[110]$ at $T = 15$ K for several $(Sr_{1-x}Ca_x)_3Ru_2O_7$ samples. This field orientation was chosen because it is the easy axis of magnetization for the majority of the materials, at least for $x > 0.3$. (See Ref. 4 for details about the $x = 1.0$ material.) The chosen temperature $T = 15$ K is well below any of the ordering temperatures, so in effect represents the $T = 0$ isotherm.

In Fig. 6(a) we see that the $H\|[110]$ data for $x = 0$ (ferromagnet at $T_c = 105$ K) show a field-induced spin reorientation transition (perhaps metamagnetic) at about 2.5 T. As can be seen from the inset of Fig. 6(b), the magnetization saturates quickly for $H\|[001]$, demonstrating once again that [001] is the easy axis. The inset of Fig. 6(b) also shows low-field detail; this indicates that there is a slight canting of the moments from [001] that pins the moment at near $M = 0$ for $H < 0.05$ T before rapidly rising to the full saturation moment in the easy direction, which is about $1.35\mu_B/$Ru. This is slightly less than the saturation moment of ferromagnetic $SrRuO_3$, which saturates for $H > 20$ T at $1.65\mu_B/$Ru.[16] The ferromagnetic domain structure in the Sr-rich samples may also play a role in the low-field magnetization. As Ca concentration is increased the [110] transitions shift somewhat nonmonotonically with increasing x to higher fields, and the 7 T moment decreases. This probably reflects a change in the easy axis orientation and that for $H > 7$ T higher-field transitions would carry the moment closer to $1.3\mu_B/$Ru. Finally, for $x = 1.0$, we see a characteristic first-order metamagnetic transition where at $H = 5.8$ T the spins, which are antiferromagnetically coupled along [110], are reoriented ferromagnetically. This transition is accompanied by a first-order transition in the magnetoresistivity from a nonmetallic to metallic state.[4]
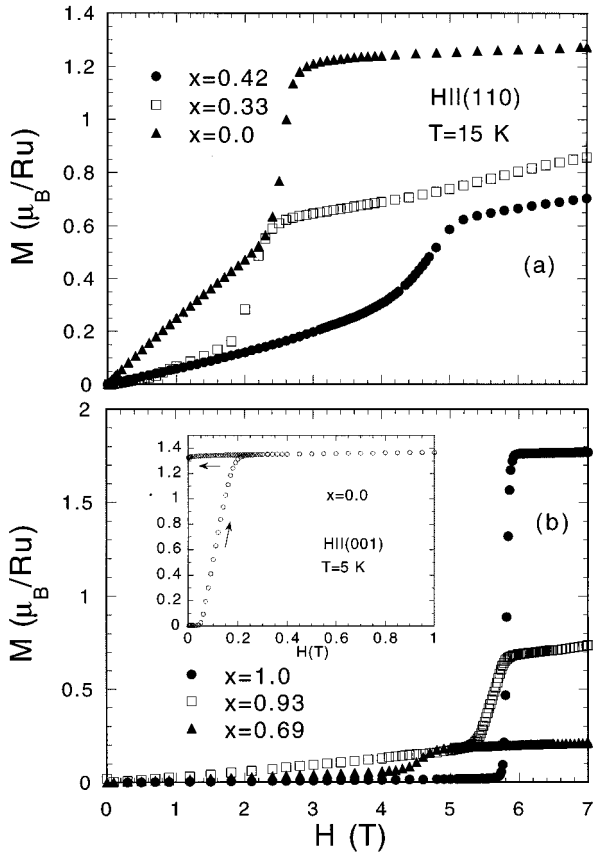
FIG. 6. Isothermal magnetization $M(H)$ to $H=7$ T for several $(Sr_{1-x}Ca_x)_3Ru_2O_7$ samples showing a trend from ferromagnetism (low x) to metamagnetic behavior ($x \approx 1.0$). The inset of (b) shows the detail of M vs H at low H for the $x=0$ ferromagnetic material along the easy axis $H\|[001]$.

V. SUMMARY OF PHASE DIAGRAM AND DISCUSSION

Because the preferred spin orientation varies with x in $(Sr_{1-x}Ca_x)_3Ru_2O_7$, it is difficult to construct a full x-T-H phase diagram. Figure 7 represents the zero-field x-T magnetic phase diagram for $(Sr_{1-x}Ca_x)_3Ru_2O_7$. The system remains ferromagnetic for $x \leq 0.4$ and is clearly antiferromagnetic for $x > 0.65$. For both regions there are two reasonably distinct transitions separating different ferromagnetic and antiferromagnetic phases, respectively. In the intermediate region $0.4 < x < 0.65$ there is some ambiguity of the spin configuration determined from these bulk macroscopic measurements. From Fig. 3(b) we see that the transition from metallic to nonmetallic electrical conductivity for $T \leq 40$ K occurs around $x \cong 0.7$. Thus the transition from low-temperature metallic to nonmetallic conductivity in $(Sr_{1-x}Ca_x)_3Ru_2O_7$ appears to be preceded by the transition from ferromagnetism to antiferromagnetism at around $x \cong 0.4$.

In all the data presented here, clearly defined resistive anomalies accompany the transition from the magnetically disordered to magnetically ordered state. This rather dramatically underscores the spin-charge coupling in these $4d$ materials, a property that may well be related to the rather large radial extent of the Ru $4d$ shell. In more conventional magnetically doped systems, such as magnetically doped metals
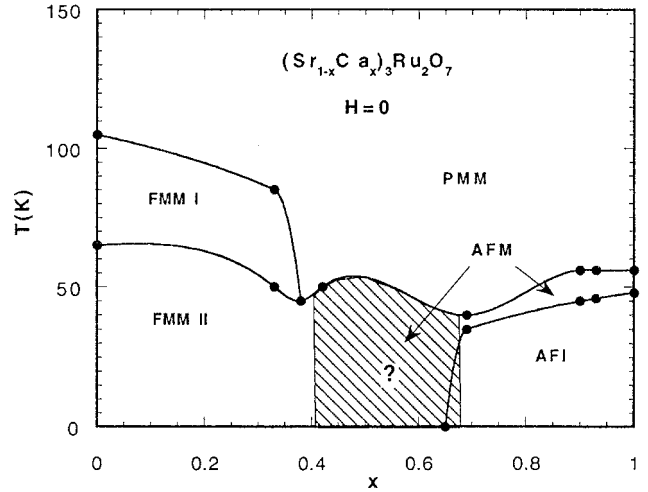

FIG. 7. Magnetic phase diagram ($H=0$) showing multiple phases for the $(Sr_{1-x}Ca_x)_3Ru_2O_7$ system. The phases from this diagram are derived from the data of Figs. 2–4.

with rare-earth impurities, the transport is dominated by the s- and p-electron bands, whereas the magnetic properties are determined primarily by localized $4f$ shells. In the transition-metal oxides, and the ruthenates in particular where s-electron character is essentially absent, the spin-charge coupling is so strong that one can almost rely on resistivity measurements to determine magnetic properties, or vice versa.

Following a prior study of mixed phases between ferromagnetic $SrRuO_3$ and strongly enhanced paramagnetic $CaRuO_3$, the data presented here summarize the extraordinarily rich array of physical properties that can be found in the Ruddlesden-Popper ruthenate series. The double-layered $(Sr_{1-x}Ca_x)_3Ru_2O_7$ system shows considerably more complexity and anisotropy than the infinite layered and more isotropic $Sr_{1-x}Ca_xRuO_3$ system. In addition to more complexity of the magnetic phase diagram, the $Sr_{1-x}Ca_xRuO_3$ system remains metallic at all measured temperatures for all x, unlike $(Sr_{1-x}Ca_x)_3Ru_2O_7$. We emphasize that the complexity is related to the much more anisotropic two-layer structure of the $n=2$ vs $n=\infty$ Ruddlesden-Popper series.

The data presented here point out the possibility of the emergence of a gap accompanying the transition from metallic ferromagnetism to metallic antiferromagnetism. To our knowledge, no comprehensive theory exists that incorporates a gap at the Fermi surface and also addresses the trend from metallic antiferromagnetic ($0.4 \leq x \leq 0.7$) to nonmetallic antiferromagnetic behavior ($x > 0.7$), particularly a theory that incorporates the rather dramatic magnetocrystalline anisotropy of these materials.

Finally, recent (unpublished) angular resolved photoemission studies[17] on our materials show features at the Fermi surface for high-symmetry directions in the Brillouin zone that, while incomplete, are consistent with the results presented here. The general trend from good metallic to poor metallic conductivity is apparent from an observed decrease of a quasiparticle peak at the Fermi energy that exists for the Sr-rich materials but is less evident for Ca-rich ($x \approx 1.0$) samples.

We expect the results presented here will help to focus attention on the further understanding of such a trend as well as a more secure theoretical explanation of the properties of materials at the crossover between metals and nonmetals and among ''bad'' metal systems in general.

[*]Also at National High Magnetic Field Laboratory, Florida State University, Tallahassee, FL 32310 and Francis Bitter Magnet Laboratory, Massachusetts Institute of Technology, Cambridge, MA 02139.

[1]For a review of transition-metal oxide physics see P. A. Cox, *Transition Metal Oxides* (Clarendon, Oxford, 1995).

[2]S. N. Ruddlesden and P. Popper, Acta Crystallogr. **11**, 54 (1958).

[3]G. Cao, S. McCall, and J. E. Crow, Phys. Rev. B **55**, R672 (1997).

[4]G. Cao, S. McCall, J. E. Crow, and R. P. Guertin, Phys. Rev. Lett. **78**, 1751 (1997).

[5]S. Ikeda, Y. Maeno, M. Nohara, and T. Fujita, Physica C **263**, 558 (1996); S. Ikeda, Y. Maeno, H. Muranishi, and T. Fujita, J. Low Temp. Phys. (to be published).

[6]R. J. Cava, H. W. Zandbergen, J. J. Krajewski, W. F. Peck, Jr., B. Batlogg, S. Carter, R. M. Fleming, O. Zhou, and L. W. Rupp, Jr., J. Solid State Chem. **116**, 1412 (1995). M. Itoh, M. Shikano, and T. Shimura, Phys. Rev. B **51**, 16 432 (1995).

[7]J. J. Randall and R. Ward, J. Am. Chem. Soc. **81**, 2629 (1959).

[8]G. Cao, S. McCall, M. Shepard, J. E. Crow, and R. P. Guertin, Phys. Rev. B **56**, 321 (1997).

[9]Y. Maeno, H. Hashimoto, K. Yoshida, S. Nishizaki, T. Fujita, J. G. Bednorz, and F. Lichtenberg, Nature (London) **372**, 532 (1994).

[10]T. M. Rice and M. Sigrist, J. Phys.: Condens. Matter **7**, C643 (1995).

[11]J. J. Neumeier, M. F. Hundley, M. G. Smith, J. D. Thompson, C. Allgeier, H. Xie, W. Yelon, and J. S. Kim, Phys. Rev. B **50**, 17 910 (1994).

[12]M. E. Fisher and J. S. Langer, Phys. Rev. Lett. **13**, 665 (1968).

[13]D. Singh (private communication).

[14]N. F. Mott, in *Metal Insulator Transitions*, 2nd ed. (Taylor and Francis, London, 1990).

[15]Y. Suezaki and H. Mori, Prog. Theor. Phys. **41**, 1177 (1968).

[16]M. Shepard (private communication).

[17]A. Puchkov (private communication).